

# Photochemically Excited, Pulsating Janus Colloidal Motors of Tunable Dynamics

Chao Zhou,<sup>†</sup> Xi Chen,<sup>†</sup> Zhiyang Han,<sup>‡</sup> and Wei Wang<sup>\*,†</sup>

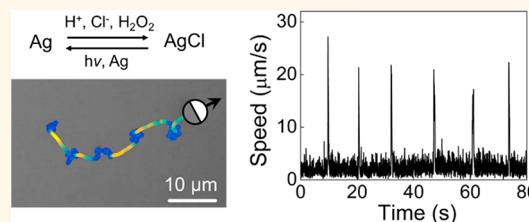
<sup>†</sup>School of Materials Science and Engineering, Harbin Institute of Technology (Shenzhen), Shenzhen, Guangdong 518055, China

<sup>‡</sup>School of Computer Science and Engineering, Harbin Institute of Technology (Shenzhen), Shenzhen, Guangdong 518055, China

**S** Supporting Information

**ABSTRACT:** Spontaneous periodicity is widely found in many biological and synthetic systems, and designing colloidal motors that mimic this feature may not only facilitate our understanding of how complexity emerges but also enable applications that benefit from a time-varying activity. However, there is so far no report on a colloidal motor system that shows controllable and spontaneous oscillation in speeds. Inspired by previous studies of oscillating silver microparticles, we report silver–poly(methyl methacrylate) microsphere Janus colloidal motors that moved, interacted with tracers, and exhibited negative gravitaxis all in an oscillatory fashion. Its dynamics, including pulsating speeds and magnitude, can be systematically modulated by varying chemical concentrations, light intensity, and the way light was applied. A qualitative mechanism is proposed to link the oscillation of Janus colloidal motors to ionic diffusiophoresis, while nonlinearity is suspected to arise from a sequence of autocatalytic decomposition of AgCl and its slow buildup in the presence of H<sub>2</sub>O<sub>2</sub> and light. The generation of light-absorbing Ag nanoparticles is suspected to be the key. This study therefore establishes a robust model system of chemically driven, oscillatory colloidal motors with clear directionality, good tunability, and an improved mechanism, with which complex, emergent phenomena can be explored.

**KEYWORDS:** *chemical oscillator, nanomotors, micromotors, Janus, nonlinear, diffusiophoresis*



Colloidal motors, synthetic microparticles that convert environmental energy into autonomous motion, represent the latest examples of stimuli-responsive materials<sup>1–4</sup> and serve as model systems to study active matters,<sup>5–8</sup> such as cells and microorganisms. On the other hand, many biological processes exhibit activities that spontaneously vary over time. Prominent examples include cardiac pacemaker cells that beat by periodically resetting their transmembrane potentials,<sup>9,10</sup> neurons with oscillating potentials that give rise to brain waves and circadian cycles,<sup>11–13</sup> and cellular oscillations during embryogenesis.<sup>14,15</sup> Synthetic colloidal motors with oscillating dynamics could help us understand and mimic these nonlinear processes. Moreover, oscillating colloidal motors could introduce new and attractive features to drug delivery or microassembly applications<sup>16–18</sup> by enabling possibilities such as periodic release of insulin or cycled annealing during particle assembly.

To drive a colloidal particle into spontaneous oscillation, however, requires special propulsion strategies. One exciting possibility comes from chemistry. Chemical reactions are often used to power colloidal motors *via* concentration gradients or bubbles,<sup>4,19–24</sup> and the vast pool of accessible chemical reactions hint at the possibility of time-variant motor activity. Indeed, simple chemical reactions, such as the decomposition of H<sub>2</sub>O<sub>2</sub> and the consequent nucleation of oxygen bubbles,

have been reported to nudge colloids into apparent “periodic” or “oscillatory” motion.<sup>25,26</sup> Moreover, nonlinear chemical systems, such as Belousov–Zhabotinsky (BZ) reactions and iodine clock, offer a more exciting and complex playground. However, although oscillating BZ gels,<sup>27–29</sup> droplets,<sup>30–32</sup> and beads<sup>33</sup> demonstrating interesting patterns and collective behaviors have been reported, most of these systems lack asymmetries that enable directional motion and do not operate at micro- or even nanoscales.

On the other hand, recent discoveries of silver-based chemical oscillations present an interesting opportunity for designing periodic colloidal motors, yet challenges remain. In these systems, the oxidation of Ag into Ag<sub>3</sub>PO<sub>4</sub> or AgCl on the surface of a microparticle<sup>34,35</sup> and its photo-decomposition back into Ag when illuminated, proceeds in a time-variant fashion. Phenomenologically, individual particles alternated between moving and stopping, while charged tracer microspheres attached and were expelled periodically from the active silver-based particles.<sup>35</sup> Two major issues stand in the way between these preliminary reports and a robust oscillating

**Received:** October 30, 2018

**Accepted:** March 27, 2019

**Published:** March 27, 2019

colloidal motor system. First, the chemically synthesized Ag or AgCl/Ag<sub>3</sub>PO<sub>4</sub> particles suffered from size polydispersity and shape irregularity, which not only caused the dynamics of oscillating particles to be sporadic in both space and time but also prevented a clear visualization of the details of their dynamics (such as directionality and orientation). Second, the preliminary mechanism given to explain the oscillatory behaviors was far from being complete or self-consistent.

Despite these limitations, pioneering studies of silver-based chemical oscillators offer a tangible framework and a source of inspiration. In this paper, we report a Janus colloidal motor that moves in aqueous solution in a pulsating manner with well-controlled dynamics and directionality. To solve the issue of polydispersity, we break the particle symmetry in a controllable fashion by half-coating a dielectric microsphere with silver. The resulting Janus colloidal motor oscillated between moving and stops in a way that is much more consistent, predictable, and clear for observation. In addition, systematic tuning of the magnitude and frequency of their pulses is achieved by varying the concentrations of a few critical chemicals as well as the light intensity. We have also made the unusual observation that turning off the light propels Janus particles into a short but powerful pulse, while intermittent illumination changed a pulsating Janus particle to pseudocontinuous motion. Finally, a qualitative mechanism is proposed at the end of the article to explain the observed motor dynamics. This study establishes a robust model system of colloidal motors with spontaneous, nonlinear activity with which future applications can be developed and complex emergent phenomena such as synchronization and chemical waves can be explored.

## RESULTS AND DISCUSSION

**Individual Dynamics of Pulsating Motors.** We first briefly introduce the fabrication process of our Janus colloidal motor and its dynamics, while more details can be found in the [Methods](#). In a typical experiment, Janus microspheres were fabricated by evaporating 50 nm of silver (Ag) on the surface of a monolayer of poly(methyl methacrylate) microspheres (PMMA) of 2.5  $\mu\text{m}$  in diameter ([Figure 1a](#)) and then suspended in solutions of H<sub>2</sub>O<sub>2</sub> (0.5 wt %) and KCl (200  $\mu\text{M}$ ) and observed from underneath with an inverted optical microscope ([Figure S1](#)). UV light of maximum power of 387 mW/cm<sup>2</sup> was generated by a mercury lamp (see [Figure S2](#) for the spectrum) and applied from above. We note that H<sub>2</sub>O<sub>2</sub>, KCl, and light are all essential ingredients for oscillatory dynamics to occur. All optical micrographs were taken on the X–Y plane where particles settled on, slightly above the bottom substrate.

When first exposed to UV light, these PMMA–Ag particles would, after a short induction period, quickly move forward and away from the Ag cap (phase 1), followed by a slow decay in speeds (phase 2). After moving forward for 1–2 s, the motor entered a relatively long refractory period of very little activity besides Brownian motion (phase 3). Soon, the next cycle of phases 1–3 kick started. [Video S1](#) and [Figure 1](#) demonstrate an example of such pulsating micromotors. A representative trajectory of one such pulsating particle is shown in [Figure 1b](#), while [Figure 1c,d](#) shows its instantaneous speeds, where the periodic oscillation in particles speeds can be clearly seen. Such an oscillation could last for 10–20 min, beyond which point particles gradually lost activity and eventually returned to Brownian motion ([Figure S3](#)). Sometimes particles were able

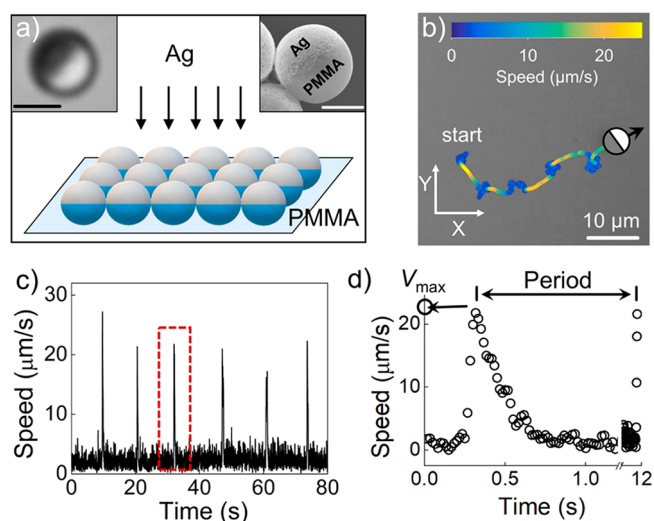


**Figure 1.** Synthesis and dynamics of pulsating colloidal motors. (a) PMMA–Ag Janus microspheres were fabricated by evaporating a thin layer of silver on a monolayer of poly(methyl-methacrylate) microspheres. Inset: Optical (top left, scale bar 2  $\mu\text{m}$ ) and scanning electron micrograph (top right, scale bar 2  $\mu\text{m}$ ) of a PMMA–Ag Janus particle. (b) Optical micrograph showing the trajectory of one PMMA–Ag particle moving away from its Ag cap for 105 s, with instantaneous speeds color-coded (see the second half of [video S1](#)). This particle is in a solution of 0.5 wt % H<sub>2</sub>O<sub>2</sub> and 200  $\mu\text{M}$  of KCl and illuminated with a light power density of 387 mW/cm<sup>2</sup>. (c) Instantaneous speeds of the pulsating PMMA–Ag motor in (b) plotted over time. (d) Magnified view of the highlighted peak in (c), showing a sharp rise and a slow decay of particle speeds and a pulse period of  $\sim 12$  s. The peak speed ( $V_{\text{max}}$ ) is labeled for reference. Note that the  $x$ -axis is broken between 1 and 12 s to show the onset of the next cycle.

to move slowly (a few  $\mu\text{m/s}$ ) away from their Ag caps between two pulses, and this can be tentatively attributed to catalytic decomposition of H<sub>2</sub>O<sub>2</sub> by Ag, as discussed in more details in [step 4'](#) in the mechanism section.

To briefly comment on the generality of this observation, Janus particles made of coating silver on other dielectric materials such as polystyrene and SiO<sub>2</sub> microspheres showed behaviors qualitatively similar to the ones made by PMMA. In addition, we confirm that visible light could also be used to achieve similar but subdued dynamics (see [Figure S4](#)). A systematic study of the particle dynamics under different wavelengths is, however, beyond the scope of this study.

**Modulating Pulses.** By judiciously choosing the right set of experimental parameters, one can design motors of a wide spectra of pulsing dynamics, ranging from powerful but less frequent beats to fast but feeble pulses. An example is given in [Figure 2a,b](#) where varying the concentrations of KCl modulated the motor dynamics. Other parameters including concentrations of H<sub>2</sub>O<sub>2</sub>, light intensity, and solution ionic strength have been systematically investigated, and data are presented in [Figure 2c–e](#). Our experiments show that a Janus motor that pulsed frequently (*i.e.*, of a small pulsing period) can be a result of a low supply of KCl ([Figure 2a](#) and [b](#)) or high supply of H<sub>2</sub>O<sub>2</sub> ([Figure 2c](#)). Furthermore, there was a significant decrease in particle speeds when the ionic strength of the solution was increased by adding KNO<sub>3</sub>, while periods remained more or less the same ([Figure 2d](#)). Such a speed decrease in elevated ionic strength has been well documented for many types of colloidal motor and is often considered a

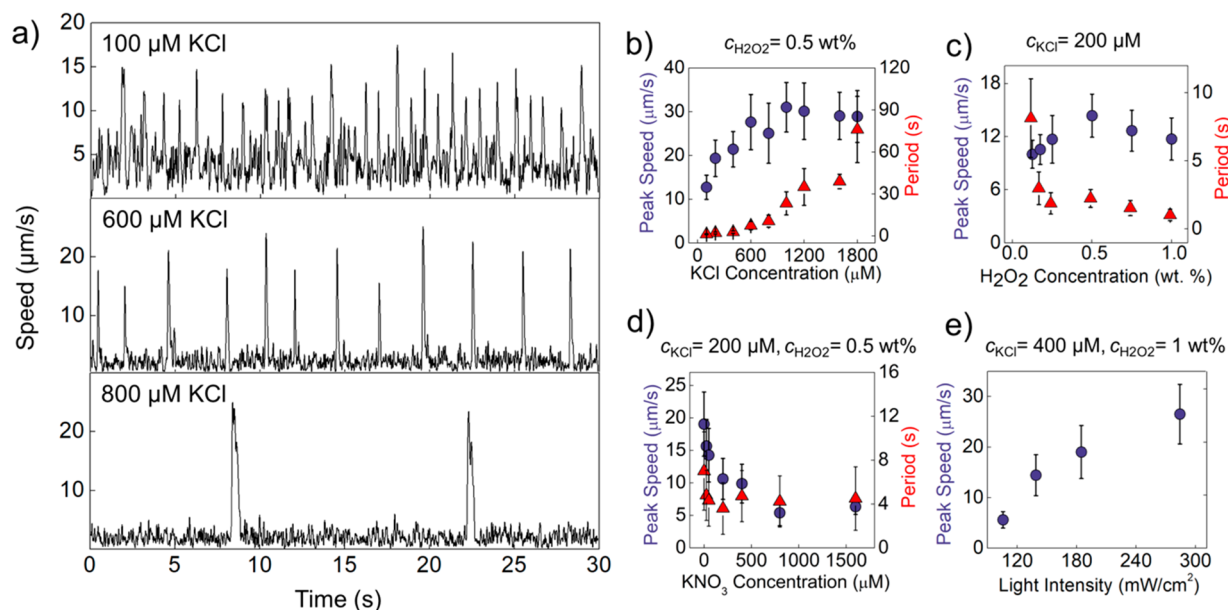


**Figure 2.** Tuning the dynamics of pulsating colloidal motors. (a) Speed profiles of pulsating PMMA–Ag motors in solutions that contain various concentrations of KCl, an essential ingredient for oscillation. All the other experimental conditions were kept the same. (b–e) Changes in the peak speeds (left y-axis, blue circles) and pulsating periods (right y-axis, red triangles) of PMMA–Ag particles by varying the concentration of KCl (b), H<sub>2</sub>O<sub>2</sub> (c), KNO<sub>3</sub> (d), and light intensity (e). Mercury lamp of 387 mW/cm<sup>2</sup> was used in (b–d), while a halogen lamp (mostly visible light) operating at various power levels was used in (e). Concentrations of other chemicals present in the solution are labeled on the top of each plot. Note that the effect on pulsating periods by varying light intensity was inconsistent across multiple experiments, and the results are therefore not given in (e). Data points in (b–e) were obtained by averaging the peak speeds or periods from speed profiles such as those shown in (a).

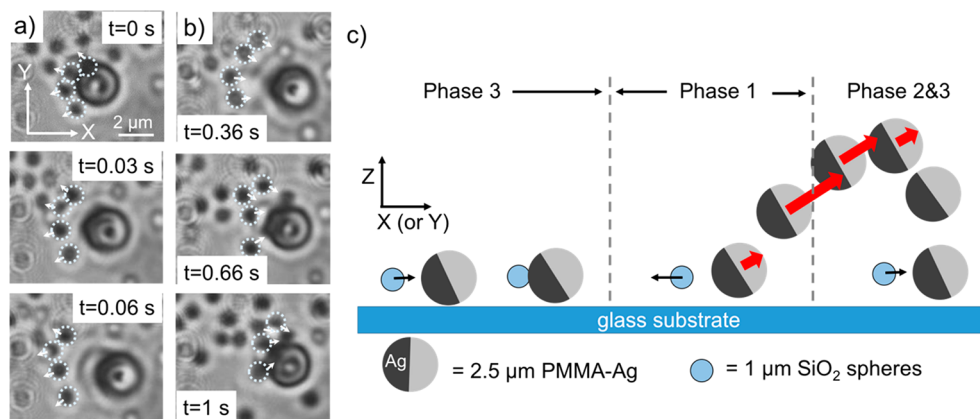


**Figure 3.** Oscillatory interactions between PMMA–Ag motors and SiO<sub>2</sub> tracer particles. (a, b) 1 μm negatively charged SiO<sub>2</sub> microspheres periodically moved away from (a) and toward (b) a PMMA–Ag motor during one cycle. Time stamps are labeled on the optical micrographs. (c) The same attraction and repulsion viewed from the side, with the corresponding phases of motion of the pulsating Janus particle. Motors often moved upward and away from the bottom substrate (negative gravitaxis) when pulsating (phase 1). The orientation of the colloidal motor shown during gravitaxis is speculative, since the clear and unambiguous visualization of the interface between two hemispheres was difficult.

hallmark of electrokinetic mechanisms (such as electrophoresis or ionic diffusiophoresis).<sup>36</sup> Notably, among the many experimental parameters that can affect pulsating dynamics, light intensity offers an option that is easily accessible and on demand. This is shown in [video S2](#) where the intensity of pulses clearly increased as the light intensity increased.

**Interaction with Tracers.** Not only did a PMMA–Ag Janus particle pulsate forward, it also attracted and repelled nearby charged tracer particles in a periodic fashion. This is demonstrated in [Figure 3](#) and [video S3](#), where a few 1 μm SiO<sub>2</sub> microspheres (zeta potential −36.3 mV) were quickly expelled from the Ag hemisphere of a 2.5 μm PMMA–Ag particle as

the Janus particle pulsed away ([Figure 3a](#)). They then slowly aggregated toward the same hemisphere ([Figure 3b](#)). The time scales associated with the two processes suggest a fast/stronger repulsion and slow/weaker attraction between tracer particles and the motor. A schematic of these two processes from a side view is given in [Figure 3c](#) in reference to the three phases of a moving Janus particle described above. Similar oscillations between the binding and release of negatively charged tracer particles by Ag microparticles have been reported previously<sup>35</sup> and were attributed to the oscillatory electric field as a result of the chemical oscillations (discussed below).



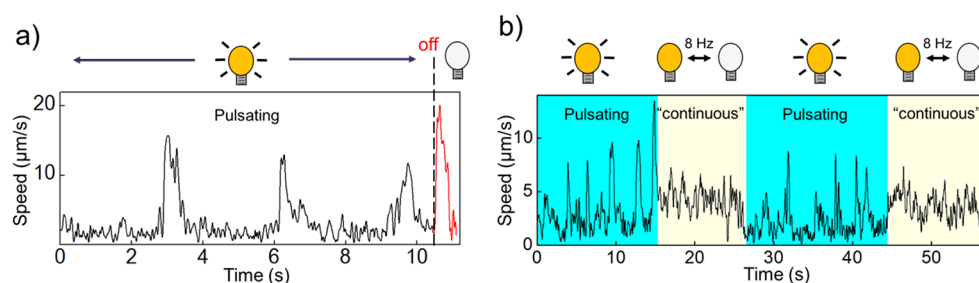


**Figure 4.** Two modes of motor dynamics *via* temporal modulation of illumination. (a) Upon turning off the light, a pulsating PMMA–Ag motor suddenly moves forward and away from the Ag cap before it stops (red peak). (b) By switching between continuous and intermittent (8 Hz) illumination, a PMMA–Ag motor switches between pulsating forward and pseudocontinuous motion, respectively.

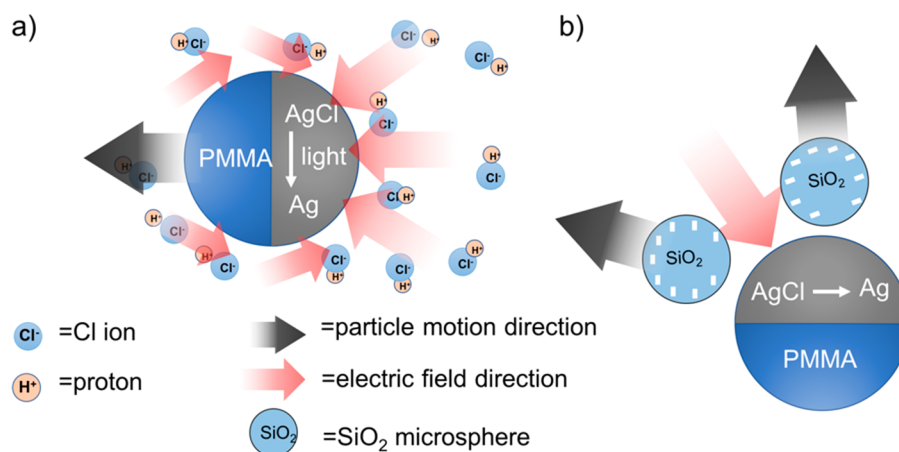


**Figure 5.** Self-diffusiophoresis of a Janus motor. (a) Photodecomposition of AgCl (eq 2) releases  $\text{H}^+$  and  $\text{Cl}^-$ , and the resulting electric field moves the Janus particle toward the uncoated side. Adapted from ref 39. (b) Self-generated electric field points inward, exerting an outward electrophoretic force on negatively charged  $\text{SiO}_2$  tracers.

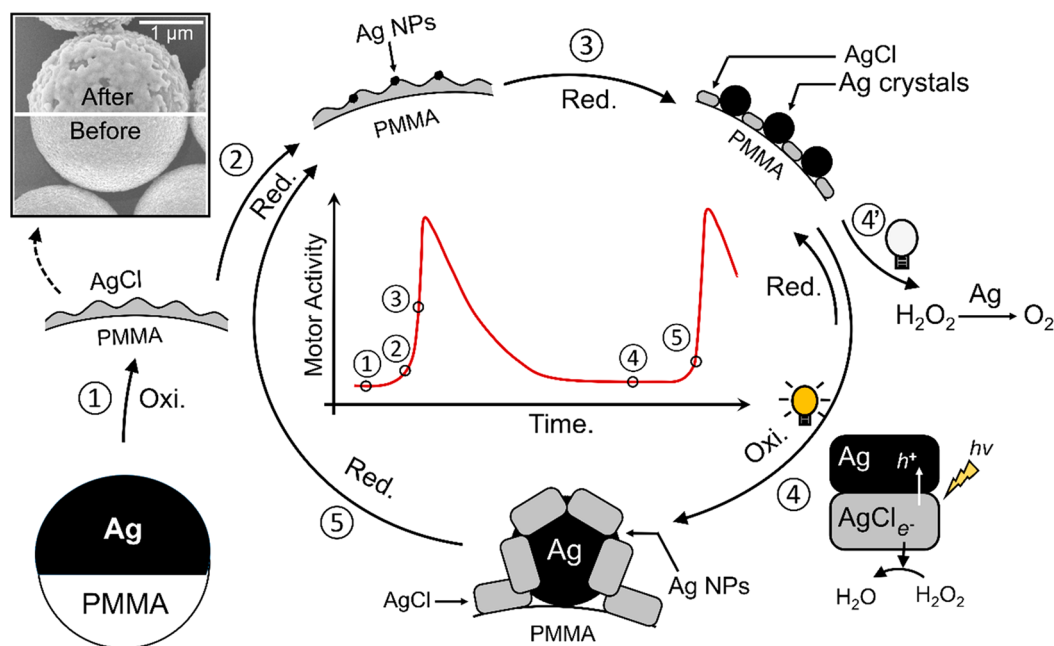
**Negative Gravitaxis.** Another interesting observation is the negative gravitaxis of Ag Janus motors (Figure 3c), inching away from the substrate as they pulsed forward (video S4) until they reached the “ceiling” that was the top of the experimental chamber. Similar negative gravitaxis has been recently reported for Pt-coated Janus particles in bulk  $\text{H}_2\text{O}_2$ <sup>37</sup> as well as PMMA–AgCl and  $\text{SiO}_2$ – $\text{TiO}_2$  Janus particles irradiated with light.<sup>38,39</sup> A likely explanation for all these observations, along with ours, is that the active cap (Ag/AgCl in our case) is heavier than both water and the other hemispheres and preferably orients downward, thus propelling the particle upward.

On the other hand, a number of previous studies have reported that phoretic colloidal motors, such as Pt-coated microspheres, did not exhibit negative gravitaxis but were preferably attached to solid–liquid interfaces such as a bottom substrate. This “docking” effect was attributed by Das<sup>40</sup> and Simmchen<sup>41</sup> to an interplay between chemical gradients and hydrodynamic effects near an interface. However, we note that the three known cases of negative gravitactic colloidal motors that move away from a bottom substrate (*i.e.*, PMMA–AgCl,  $\text{SiO}_2$ – $\text{TiO}_2$ , and the current study) all produce ionic species when operating. This suggests that whether a phoretic colloidal motor prefers to be fixated to a solid–liquid interface or moving away from it could be mechanism dependent, with electrostatic/electrokinetic effects being an important factor.

Note that although a significant percentage of these Janus particles moved out of focus in our experiments when activated by light, some remained pulsating near the substrate, thus

enabling in-plane optical tracking that made much of the current study possible. This is likely due to an inhomogeneous distribution of particle properties and/or the fluctuation of their Ag cap orientation that interrupts a continuous upward motion.

**Switching between a Pulsating and Continuous Motor.** For all of the previous sections, light was always applied continuously throughout the experiments. In fact, no oscillation or activity beyond Brownian motion was observed if the experiments were carried out in darkness or in weak lighting conditions. One therefore expects light to be a necessary ingredient in powering motors and that a pulsating motor would stop immediately (due to low Reynolds number) when light is removed. On the contrary, as Figure 4a and video S5 clearly show, a pulsating motor surprisingly pulsed one final time (away from the Ag cap) as soon as the light was turned off or significantly weakened. Although its activity was lost after this single pulse, by rapidly switching light on and off (*e.g.*, at a few Hz), a Janus particle pulsed forward at a similar frequency to that of light triggers. For example, Figure 4b shows a speed profile of a Janus particle illuminated with light of an on/off frequency of 8 Hz at a duty cycle of 50% (see the Methods for details). As a result of such rapid pulsating forward, a Janus particle essentially moved in a pseudocontinuous fashion. Therefore, switching between a continuous and intermittent lighting switches a Janus particle between a pulsation mode and a pseudocontinuous motion, respectively (video S5, second half). We note that the switching frequency of 8 Hz was chosen somewhat arbitrarily, and a range of

Scheme 1. Tentative Mechanism for Motor Oscillation<sup>a</sup>

<sup>a</sup>The coated materials on the surface of a PMMA–Ag Janus particle cycle between Ag and AgCl. Detailed descriptions of each step are given in the main text. Two SEM micrographs are stitched together at the top left corner to compare the surface morphology of the Ag hemisphere before and after exposure to the solution and light. Variations of particle speeds over time during this cycle are presented at the center of the scheme, and the numbers labeled on the speed plot match the numbering of steps.

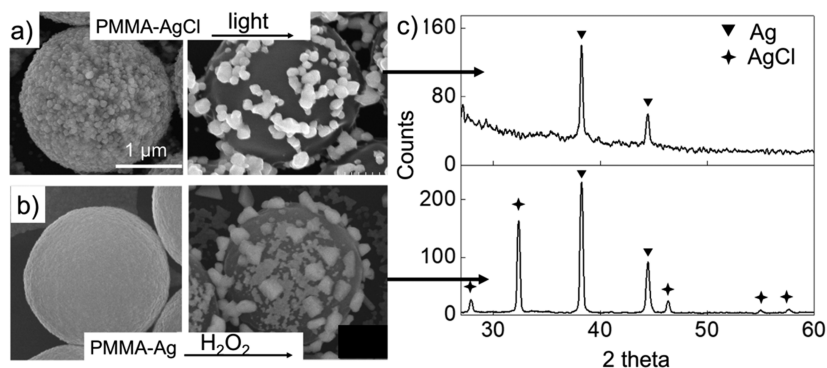


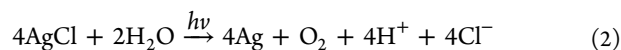
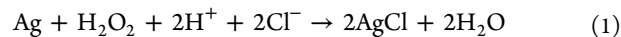
**Figure 6.** Characterizing a Janus particle after conversion. (a, b) Scanning electron micrographs of a Janus particle before (left) and after (right) the labeled reactions. Scale bar applies to all four panels. (c) X-ray diffraction patterns of the products from reactions in (a) and (b). In order to obtain enough samples for XRD characterization, a monolayer of Janus particles on a piece of silicon wafer was exposed to the respective solution and lighting condition for an extended period of time. More details are given in the [Methods](#).

frequencies from  $\sim 1$  Hz to tens of Hz could achieve a similar effect. Dependence on switching frequencies will be further explored in a future study.

**Mechanism for Pulsating Motion.** The dynamics of a pulsating Ag Janus particle, along with its oscillatory interaction with nearby tracer particles, suggest an interplay between nonlinear chemical kinetics and electrokinetics. In this section, we propose a qualitative mechanism to tentatively explain how oscillation appears and how it drives a particle to move. In addition, we attempt to use this mechanism to explain the effect of varying experimental parameters on particle dynamics (Figure 2) as well as the surprising pulse when light was turned off (Figure 4).

Our mechanism is developed on the basis of an early study of a Ag–AgCl oscillatory chemical system by Ibele *et al.*, who

proposed a conversion between Ag and AgCl as the main driving force for the oscillation they observed:<sup>35</sup>



Importantly, eqs 1 and 2 and the associated release and consumption of ions power particle motion *via* a phoretic mechanism termed ionic self-diffusiophoresis (Figure 5a).<sup>42–45</sup> For example, eq 2 releases from the particle surface protons and  $\text{Cl}^-$ , whose difference in diffusivity generates an inward electric field.<sup>46</sup> This self-generated electric field couples to the negative surface charges of the PMMA–AgCl particles (see the [Methods](#) for zeta potential measurements) and pushes the particle toward the uncoated side. Negatively charged tracer particles nearby are also repelled by this electric field (Figure

5b). We note that although eq 1 reverses everything and is supposed to cause the Janus particle to reverse its course, we suspect eq 1 to be much slower and the force much weaker (see the time scales associated with Figure 3a and b). The possible contribution of substrate electroosmosis is eliminated by examining particle dynamics in the bulk solution with the help of acoustic levitation (see the Supporting Information for details).

Connecting the self-diffusiophoresis to the oscillating speed profile of a Janus motor requires a more careful look at the reaction kinetics beyond eq 1 and 2. Specifically, oscillation in activity is often induced by competing processes that involve autocatalytic processes and feedback loops, such as those exhibited by BZ reaction<sup>47–49</sup> and cardiac pacemaker cells.<sup>9,50</sup> These details are, however, missing from previous studies of Ag-based oscillatory colloidal particles.<sup>35</sup> In the following, we propose a mechanism to qualitatively understand particle motion during one pulse period, as well as why reactions oscillate rather than reaching a steady state. This tentative mechanism, illustrated in Scheme 1, is based on a combination of material characterization, experimental observations, literature reports, and our hypothesis. It is broken down into the following five steps as follows:

(1) *Induction.* After Ag Janus particles were mixed with the experimental solution, the solution surface was converted to primarily AgCl, as supported by scanning electron microscopy (SEM, Figure 6b) and X-ray diffraction (XRD, Figure 6c). The SEM inset in Scheme 1 also shows a patched and rough surface after this conversion.

(2) *Onset of Speed Peak.* The photodecomposition of AgCl (eq 2) produced Ag nanoparticles that enabled strong adsorption of visible light.<sup>51</sup> The absorption of visible light by Janus motors in our experiment was supported by an experiment where the motor still moved (albeit with a lower speed) after the UV component in the light was filtered out (Figure S4), as well as two recent studies of Ag/AgCl nanomotors moving under visible light.<sup>39,52</sup>

(3) *Development of Speed Peaks.* As more Ag nanoparticles were produced, more photochemical “hotspots” accelerated the decomposition of AgCl in a way similar to that of autocatalysis. A dramatic increase in the reaction rate consequently led to fast and directional motion based on self-diffusiophoresis. Soon, however, the consumption of AgCl reduced the amount of available AgCl on the particle surface. In addition, Ag nanoparticles grew into larger crystals (see Figure 6a) that stopped serving as a light absorber but rather blocked AgCl underneath from further reactions. Particle speeds therefore decreased. Steps 2 and 3 are the core steps explaining the rise and fall of a peak in particle speeds.

(4) *Refractory Periods.* As the autocatalytic episode of AgCl decomposition comes to an end, there is a mixture of AgCl and Ag on the particle surface. Because AgCl is a n-type semiconductor, under light the photogenerated holes are collected by the attached Ag particles and induced the photoelectrochemical oxidation of Ag into AgCl. H<sub>2</sub>O<sub>2</sub>, on the other hand, serves as an electron scavenger and is reduced into H<sub>2</sub>O on the AgCl surface. As a result, there was a steady buildup of AgCl on the particle surface (supported by SEM in Figure 6b and XRD in Figure 6c), which is suspected to be responsible for the refractive period of a Janus particle between its two pulses.

(4') *Ag-Catalyzed H<sub>2</sub>O<sub>2</sub> Decomposition.* This sidetrack focuses on the surprising pulse of a Janus motor when light was

turned off (Figure 4a). Since Ag is known to be a good catalyst for decomposing H<sub>2</sub>O<sub>2</sub> into O<sub>2</sub>,<sup>53,54</sup> Ag crystals on a particle surface could, in the absence of light, catalyze this reaction, instead of being photo-oxidized into AgCl as suggested in step 4. The resulting diffusiophoresis could propel the particle away from the Ag-coated side, giving rise to a pulse. This quick motion was, however, not sustainable since the surface of Ag crystals could be quickly converted by H<sub>2</sub>O<sub>2</sub> into AgCl. The above hypothesis is indirectly supported by a simple experiment where, upon addition of H<sub>2</sub>O<sub>2</sub> to an aqueous suspension of PMMA–Ag Janus particles, they immediately moved away from the Ag side but soon stopped.

(5) *The Next Pulse.* As more AgCl was produced and covered much of the Ag crystals, the remaining Ag patches became small enough to behave again as nanoparticles exhibiting plasmonic resonance in a way similar to that of steps 2 and 3, giving rise to the next pulse in particle speeds.

The key to understanding why a motor continues with these cycles rather than reaching an equilibrium is to consider that, unlike homogeneous reactions in aqueous phase, the reaction rates in the present experiments are not only controlled by the availability of chemical species but also by their states. More specifically, the autocatalytic decomposition of AgCl was only enabled when Ag nanoparticles were present, while larger Ag crystals removed holes and facilitated the exactly opposite reaction, *i.e.*, the generation of AgCl. Therefore, our proposed mechanism consists of positive feedback that is the autocatalysis of AgCl decomposition, negative feedback that limits the reaction rate by the availability of AgCl, and finally a slow reaction that restores the level of AgCl and prepares it for the next pulse.

Based on this mechanism, we can tentatively explain the effect of experimental parameters described in Figure 2. For example, a higher concentration of H<sub>2</sub>O<sub>2</sub> increases the rate, but not the total amount, of AgCl buildup in step 4 and, therefore, reduced the wait time between two pulses without significantly affecting particle speeds (Figure 2c). Similarly, a higher concentration of Cl<sup>−</sup> shifted the competition between the buildup and decomposition of AgCl in step 4, producing more AgCl at the end but took longer time to do so. This, in turn, resulted in more intense pulses with longer periods (Figure 2b). At significantly higher Cl<sup>−</sup> concentrations, though, the elevated ionic strength undermined the electrokinetic mechanism in a way similar to that of KNO<sub>3</sub>, and particle speeds reached a plateau. Since the particle moved primarily because of the photodecomposition of AgCl in steps 2 and 3, more intense light accelerated this process and produced a larger ionic flux, which gave rise to a larger peak speed (Figure 2e).

Although this proposed mechanism could, at a superficial and qualitative level, explain the oscillatory dynamics of a pulsating Janus motor, it contains some untested hypothesis and is not without limitations. For example, we have not taken into account the diffusion of chemical species. The reasoning is that although many oscillatory systems rely on a mismatch between reaction-diffusion processes, motors are hardly limited by diffusion when they move at a speed on the order of 10 μm/s and can thus be replenished easily. In addition, the actual kinetics of eqs 1 and 2 most likely contain pathways with charged or neutral intermediates. This detail could alter the mechanism we have proposed but has not been mapped in the current study. Moreover, although the generation and growth of Ag nanoparticles during the oscillation seems intuitive, its *in situ* observation is challenging. Furthermore, it would be



extremely helpful to measure the distributions of chemical species and electric fields, and the flow profiles, around an oscillating Janus particle. Experimental efforts on this subject are underway, while numerical and analytical modeling could prove useful too. These issues require careful and lengthy studies and will be explored in more depth and more systematically in a future study.

## CONCLUSION

To summarize, we have developed a Janus colloidal motor with an oscillating temporal pattern of behaviors. When illuminated with light and exposed to  $\text{H}_2\text{O}_2$  and  $\text{Cl}^-$ , PMMA–Ag Janus microspheres exhibited highly periodic motion that consists of a fast then decelerating phase away from the Ag cap followed by a refractive phase. Not only do they pulse forward, they also moved upward and against gravity (negative gravitaxis), likely due to a heavy but active cap. Pulsing frequency (as high as a few hertz) and magnitude (peak speeds as high as  $\sim 30 \mu\text{m/s}$ ) can be fine-tuned *via* chemical concentrations. Moreover, not only can light modulate how fast a motor moves, the exact way light is applied can also determine whether it pulsates or moves “continuously”. A tentative mechanism of its oscillating dynamics is proposed based on a chemical oscillation between fast and autocatalytic reduction and slow oxidation on the Ag/AgCl-coated hemisphere. However, a more careful examination and *in situ* characterization of the material composition, surface morphology, chemical distributions, flow profiles, and other properties of a pulsating Janus particle is needed to further our understanding.

Looking forward, a pulsating chemical oscillator operating at microscale or even smaller, similar to a cardiac pacemaker cell, could potentially function as a central clock unit in regulating the dynamics of a large assembly of micromachines and form the basis for a special type of stimuli-responsive, biomimetic material. Importantly, the fact that the dynamics of this pulsating chemical oscillator can be tuned systematically and *in situ* enables on-demand designs of nonlinear systems of a wide range of characteristics. Although we have mostly focused on single particle dynamics in this paper, interesting nonlinear dynamics<sup>55</sup> among these chemical oscillators such as collective synchronization<sup>56</sup> and chemical waves<sup>57</sup> are exciting topics that are being pursued and will be reported separately.

## METHODS

**Motor Experiments.** In a typical experiment, a mixed aqueous suspension of PMMA–Ag particles and chemicals was transferred by capillary effect into a rectangular shaped capillary tube made of glass (Vitrocom No. 3520-050, thickness of  $\sim 200 \mu\text{m}$ ) and observed from underneath with an inverted optical microscope (Olympus IX71), and light was applied from the top (see Figure S1 for setup). An upright microscope configuration can also be used. Due to gravity, Janus particles naturally sedimented to the bottom of the capillary tube, where the focal plane was commonly chosen. However, in cases where colloidal particles on other planes needed to be examined, such as in gravitaxis experiment or levitation experiment, the focus knob on the microscope could be manually adjusted to refocus on a different plane. Different light sources can be accessed by switching the mounted lamp from a halogen lamp to a mercury lamp (see Figure S2 for spectra of these two light sources) by applying optical filters that modulate light wavelength and intensity or by adjusting lamp power levels. Videos were recorded with a CMOS camera (FLIR GS3-U3-41C6C-C, Point Grey) typically at 30 frames per second (fps). They were later processed by imageJ and analyzed by MATLAB to find the coordinates of each particle, which were used to calculate instantaneous particle speeds.

The experiments where light was applied intermittently were carried out with a LED UV light source (Thorlab M365LP1-C1) with a peak wavelength at 365 nm. Its controller is connected to a function generator which triggered its on and off.

**Surface Characterization.** A monolayer of PMMA–Ag particles was prepared on a silicon wafer, broken into small pieces, and used for three separate tests. First, to examine the surface morphology of a PMMA–Ag Janus particle shortly after exposure to an oxidizing solution, the wafer piece with PMMA–Ag particles was immersed in a solution of 1 wt %  $\text{H}_2\text{O}_2$  and 400  $\mu\text{M}$  KCl. SEM images before and after oxidization are stitched to give the inset image in Scheme 1. Second, in order to confirm the occurrence of eq 1 in our experiments, PMMA–Ag particles was immersed in a solution of 0.5 wt %  $\text{H}_2\text{O}_2$  and 200  $\mu\text{M}$  KCl in the absence of light for 20 min. The particles on wafer were then cleaned with DI water and SEM (Figure 6b), and XRD (Figure 6c, bottom) characterizations were carried out. Finally, to investigate eq 2, PMMA–AgCl particles were synthesized by immersing a monolayer of PMMA–Ag particles into an aqueous solution containing 0.01 mol/L  $\text{FeCl}_3$  solutions and 0.025 mol/L polyvinylpyrrolidone (PVP, monomer concentration) at room temperature for 20 min. As synthesized PMMA–AgCl particles were washed by DI water and irradiated with UV light ( $103 \text{ mW/cm}^2$ ) in water for 30 min (no other chemicals). The particles on wafer were then washed by DI water before (Figure 6a) and after XRD (Figure 6c, top) characterizations.

Zeta potential measurements were carried out with Malvern Zetasizer for  $\text{SiO}_2$  tracer particles ( $-36.3 \text{ mV}$ ), PMMA microspheres ( $-49.1 \text{ mV}$ ), and PMMA–AgCl microparticles ( $-35.1 \text{ mV}$ ). Although we were not able to directly measure the zeta potential on the AgCl hemisphere of a Janus particle, it is inferred to be negative from that of a PMMA and a PMMA–AgCl particle.

## ASSOCIATED CONTENT

### Supporting Information

The Supporting Information is available free of charge on the ACS Publications website at DOI: 10.1021/acsnano.8b08276.

Video S1: An example of oscillating motors (AVI)

Video S2: Oscillating motors modulated on-the-fly, remotely, and instantaneously by varying light intensity (AVI)

Video S3: Periodic attraction and repulsion between active Janus particles and negative charged tracer spheres (AVI)

Video S4: Pulsating motor moving from the bottom to the top of the cell (AVI)

Video S5: Photoswitching between pulsing and continuous motions (AVI)

Experimental setup and light spectra used, motor dynamics over long time, the effect of light wavelength on motor dynamics, and experiments to eliminate electroosmosis (PDF)

## AUTHOR INFORMATION

### Corresponding Author

\*E-mail: weiwangsz@hit.edu.cn, wwang.hitsz@gmail.com.

### ORCID

Wei Wang: 0000-0003-4163-3173

### Notes

The authors declare no competing financial interest.

## ACKNOWLEDGMENTS

We are deeply grateful for the helpful discussions with Profs. Thomas Mallouk, Ayusman Sen, Darrell Velegol, Hepeng Zhang, John Gibbs, Raymond Kapral, and Zexin Zhang. This project is financially supported by the National Natural Science

Foundation of China (11774075 and 11402069), Natural Science Foundation of Guangdong Province (No. 2017B030306005), and the Science Technology and Innovation Program of Shenzhen (JCYJ20170307150031119).

## REFERENCES

- (1) Wang, J. *Nanomachines: Fundamentals and Applications*; John Wiley & Sons: Hoboken, NJ, 2013.
- (2) Mallouk, T. E.; Sen, A. Powering Nanorobots. *Sci. Am.* **2009**, *300*, 72–77.
- (3) Zhang, J.; Luijten, E.; Grzybowski, B. A.; Granick, S. Active Colloids with Collective Mobility Status and Research Opportunities. *Chem. Soc. Rev.* **2017**, *46*, 5551–5569.
- (4) Wang, W.; Duan, W.; Ahmed, S.; Mallouk, T. E.; Sen, A. Small Power: Autonomous Nano- and Micromotors Propelled by Self-Generated Gradients. *Nano Today* **2013**, *8*, 531–554.
- (5) Cates, M. E.; MacKintosh, F. C. Active Soft Matter. *Soft Matter* **2011**, *7*, 3050–3051.
- (6) Marchetti, M. C.; Joanny, J.-F.; Ramaswamy, S.; Liverpool, T. B.; Prost, J.; Rao, M.; Simha, R. A. Hydrodynamics of Soft Active Matter. *Rev. Mod. Phys.* **2013**, *85*, 1143.
- (7) Yeomans, J. M. Nature's Engines: Active Matter. *Europhys. News* **2017**, *48*, 21–25.
- (8) Needleman, D.; Dogic, Z. Active Matter at the Interface between Materials Science and Cell Biology. *Nat. Rev. Mater.* **2017**, *2*, 17048.
- (9) DiFrancesco, D. Pacemaker Mechanisms in Cardiac Tissue. *Annu. Rev. Physiol.* **1993**, *55*, 455–472.
- (10) Hutcheon, B.; Yarom, Y. Resonance, Oscillation and the Intrinsic Frequency Preferences of Neurons. *Trends Neurosci.* **2000**, *23*, 216–222.
- (11) Colwell, C. S. Linking Neural Activity and Molecular Oscillations in the SCN. *Nat. Rev. Neurosci.* **2011**, *12*, 553.
- (12) Lopes da Silva, F. Neural Mechanisms Underlying Brain Waves: From Neural Membranes to Networks. *Electroencephalogr. Clin. Neurophysiol.* **1991**, *79*, 81–93.
- (13) Metherate, R.; Cox, C. L.; Ashe, J. H. Cellular Bases of Neocortical Activation: Modulation of Neural Oscillations by the Nucleus Basalis and Endogenous Acetylcholine. *J. Neurosci.* **1992**, *12*, 4701–4711.
- (14) Solon, J.; Kaya-Copur, A.; Colombelli, J.; Brunner, D. Pulsed Forces Timed by a Ratchet-Like Mechanism Drive Directed Tissue Movement During Dorsal Closure. *Cell* **2009**, *137*, 1331–1342.
- (15) Dierkes, K.; Sumi, A.; Solon, J.; Salbreux, G. Spontaneous Oscillations of Elastic Contractile Materials with Turnover. *Phys. Rev. Lett.* **2014**, *113*, 148102.
- (16) Ebbens, S. Active Colloids: Progress and Challenges Towards Realising Autonomous Applications. *Curr. Opin. Colloid Interface Sci.* **2016**, *21*, 14–23.
- (17) Li, J.; de Ávila, B. E.-F.; Gao, W.; Zhang, L.; Wang, J. Micro/Nanorobots for Biomedicine: Delivery, Surgery, Sensing, and Detoxification. *Sci. Robot.* **2017**, *2*, No. eaam6431.
- (18) Medina-Sánchez, M.; Magdanz, V.; Guix, M.; Fomin, V. M.; Schmidt, O. G. Swimming Microrobots: Soft, Reconfigurable, and Smart. *Adv. Funct. Mater.* **2018**, *28*, 1707228.
- (19) Dey, K. K.; Sen, A. Chemically Propelled Molecules and Machines. *J. Am. Chem. Soc.* **2017**, *139*, 7666–7676.
- (20) Sánchez, S.; Soler, L.; Katuri, J. Chemically Powered Micro- and Nanomotors. *Angew. Chem., Int. Ed.* **2015**, *54*, 1414–1444.
- (21) Moo, J. G. S.; Pumera, M. Chemical Energy Powered Nano/Micro/Macromotors and the Environment. *Chem. - Eur. J.* **2015**, *21*, 58–72.
- (22) Robertson, B.; Huang, M.-J.; Chen, J.-X.; Kapral, R. Synthetic Nanomotors: Working Together through Chemistry. *Acc. Chem. Res.* **2018**, *51*, 2355–2364.
- (23) Li, J.; Rozen, I.; Wang, J. Rocket Science at the Nanoscale. *ACS Nano* **2016**, *10*, 5619–5634.
- (24) Xu, B.; Mei, Y. Tubular Micro/Nanoengines: Boost Motility in a Tiny World. *Sci. Bull.* **2017**, *62*, 525–527.
- (25) Solovev, A. A.; Mei, Y.; Bermúdez Ureña, E.; Huang, G.; Schmidt, O. G. Catalytic Microtubular Jet Engines Self-Propelled by Accumulated Gas Bubbles. *Small* **2009**, *5*, 1688–1692.
- (26) Nakata, S.; Nomura, M.; Yamamoto, H.; Izumi, S.; Suematsu, N. J.; Ikura, Y.; Amemiya, T. Periodic Oscillatory Motion of a Self-Propelled Motor Driven by Decomposition of H<sub>2</sub>O<sub>2</sub> by Catalase. *Angew. Chem.* **2017**, *129*, 879–882.
- (27) Kuksenok, O.; Dayal, P.; Bhattacharya, A.; Yashin, V. V.; Deb, D.; Chen, I. C.; Van Vliet, K. J.; Balazs, A. C. Chemo-Responsive, Self-Oscillating Gels That Undergo Biomimetic Communication. *Chem. Soc. Rev.* **2013**, *42*, 7257–7277.
- (28) Yoshida, R.; Takahashi, T.; Yamaguchi, T.; Ichijo, H. Self-Oscillating Gel. *J. Am. Chem. Soc.* **1996**, *118*, 5134–5135.
- (29) Yoshida, R. Self-Oscillating Gels Driven by the Belousov-Zhabotinsky Reaction as Novel Smart Materials. *Adv. Mater.* **2010**, *22*, 3463–3483.
- (30) Suematsu, N. J.; Mori, Y.; Amemiya, T.; Nakata, S. Oscillation of Speed of a Self-Propelled Belousov-Zhabotinsky Droplet. *J. Phys. Chem. Lett.* **2016**, *7*, 3424–3428.
- (31) Thutupalli, S.; Herminghaus, S. Tuning Active Emulsion Dynamics via Surfactants and Topology. *Eur. Phys. J. E: Soft Matter Biol. Phys.* **2013**, *36*, 91.
- (32) Torbensen, K.; Rossi, F.; Ristori, S.; Abou-Hassan, A. Chemical Communication and Dynamics of Droplet Emulsions in Networks of Belousov-Zhabotinsky Micro-Oscillators Produced by Microfluidics. *Lab Chip* **2017**, *17*, 1179–1189.
- (33) Taylor, A. F.; Tinsley, M. R.; Wang, F.; Huang, Z.; Showalter, K. Dynamical Quorum Sensing and Synchronization in Large Populations of Chemical Oscillators. *Science* **2009**, *323*, 614–617.
- (34) Altemose, A.; Sánchez-Farrán, M. A.; Duan, W.; Schulz, S.; Borhan, A.; Crespi, V. H.; Sen, A. Chemically-Controlled Spatiotemporal Oscillations of Colloidal Assemblies. *Angew. Chem.* **2017**, *129*, 7925–7929.
- (35) Ibele, M. E.; Lammert, P. E.; Crespi, V. H.; Sen, A. Emergent, Collective Oscillations of Self-Mobile Particles and Patterned Surfaces under Redox Conditions. *ACS Nano* **2010**, *4*, 4845–4851.
- (36) Paxton, W. F.; Baker, P. T.; Kline, T. R.; Wang, Y.; Mallouk, T. E.; Sen, A. Catalytically Induced Electrokinetics for Motors and Micropumps. *J. Am. Chem. Soc.* **2006**, *128*, 14881–14888.
- (37) Campbell, A. I.; Ebbens, S. J. Gravitaxis in Spherical Janus Swimming Devices. *Langmuir* **2013**, *29*, 14066–14073.
- (38) Singh, D. P.; Uspal, W. E.; Popescu, M. N.; Wilson, L. G.; Fischer, P. Photogravitactic Microswimmers. *Adv. Funct. Mater.* **2018**, *28*, 1706660.
- (39) Zhou, C.; Zhang, H.; Tang, J.; Wang, W. Photochemically Powered AgCl Janus Micromotors as a Model System to Understand Ionic Self-Diffusiophoresis. *Langmuir* **2018**, *34*, 3289–3295.
- (40) Das, S.; Garg, A.; Campbell, A. I.; Howse, J.; Sen, A.; Velegol, D.; Golestanian, R.; Ebbens, S. J. Boundaries Can Steer Active Janus Spheres. *Nat. Commun.* **2015**, *6*, 8999.
- (41) Simmchen, J.; Katuri, J.; Uspal, W. E.; Popescu, M. N.; Tasinkevych, M.; Sánchez, S. Topographical Pathways Guide Chemical Microswimmers. *Nat. Commun.* **2016**, *7*, 10598.
- (42) Velegol, D.; Garg, A.; Guha, R.; Kar, A.; Kumar, M. Origins of Concentration Gradients for Diffusiophoresis. *Soft Matter* **2016**, *12*, 4686–4703.
- (43) Popescu, M. N.; Uspal, W. E.; Dietrich, S. Self-Diffusiophoresis of Chemically Active Colloids. *Eur. Phys. J.: Spec. Top.* **2016**, *225*, 2189–2206.
- (44) Moran, J. L.; Posner, J. D. Phoretic Self-Propulsion. *Annu. Rev. Fluid Mech.* **2017**, *49*, 511–540.
- (45) Anderson, J. L. Colloid Transport by Interfacial Forces. *Annu. Rev. Fluid Mech.* **1989**, *21*, 61–99.
- (46) Kline, T. R.; Iwata, J.; Lammert, P. E.; Mallouk, T. E.; Sen, A.; Velegol, D. Catalytically Driven Colloidal Patterning and Transport. *J. Phys. Chem. B* **2006**, *110*, 24513–24521.
- (47) Vanag, V. K.; Yang, L.; Dolnik, M.; Zhabotinsky, A. M.; Epstein, I. R. Oscillatory Cluster Patterns in a Homogeneous Chemical System with Global Feedback. *Nature* **2000**, *406*, 389.



- (48) Yang, L.; Dolnik, M.; Zhabotinsky, A. M.; Epstein, I. R. Oscillatory Clusters in a Model of the Photosensitive Belousov-Zhabotinsky Reaction System with Global Feedback. *Phys. Rev. E: Stat. Phys., Plasmas, Fluids, Relat. Interdiscip. Top.* **2000**, *62*, 6414.
- (49) Epstein, I. R. Coupled Chemical Oscillators and Emergent System Properties. *Chem. Commun.* **2014**, *50*, 10758–10767.
- (50) Tsien, R.; Kass, R.; Weingart, R. Cellular and Subcellular Mechanisms of Cardiac Pacemaker Oscillations. *J. Exp. Biol.* **1979**, *81*, 205–215.
- (51) Tejada, J.; Shevchik, N.; Braun, W.; Goldmann, A.; Cardona, M. Valence Bands of AgCl and AgBr: UV Photoemission and Theory. *Phys. Rev. B* **1975**, *12*, 1557.
- (52) Wang, X.; Baraban, L.; Nguyen, A.; Ge, J.; Misko, V. R.; Tempere, J.; Nori, F.; Formanek, P.; Huang, T.; Cuniberti, G. High-Motility Visible Light-Driven Ag/AgCl Janus Micromotors. *Small* **2018**, *14*, 1803613.
- (53) Bagg, J. The Catalytic Decomposition of Hydrogen Peroxide Solutions by Single Crystals of Silver. *Aust. J. Chem.* **1962**, *15*, 201–210.
- (54) Laursen, A. B.; Man, I. C.; Trinhammer, O. L.; Rossmeisl, J.; Dahl, S. The Sabatier Principle Illustrated by Catalytic H<sub>2</sub>O<sub>2</sub> Decomposition on Metal Surfaces. *J. Chem. Educ.* **2011**, *88*, 1711–1715.
- (55) Sagués, F.; Epstein, I. R. Nonlinear Chemical Dynamics. *Dalton Trans.* **2003**, 1201–1217.
- (56) Toiya, M.; González-Ochoa, H. O.; Vanag, V. K.; Fraden, S.; Epstein, I. R. Synchronization of Chemical Micro-Oscillators. *J. Phys. Chem. Lett.* **2010**, *1*, 1241–1246.
- (57) Kapral, R.; Showalter, K. *Chemical Waves and Patterns*; Springer Science & Business Media: Berlin, 2012.